

Atom Localization in two and three dimensions via level populations in an M-type atomic system

Nilesh Chaudhari and Amarendra K Sarma*

Department of Physics, Indian Institute of Technology Guwahati, Guwahati-781039, Assam, India

(Dated: March 23, 2022)

Schemes for two-dimensional (2D) and three-dimensional (3D) atomic states localization in a five-level M-type system using standing-wave laser fields are presented. In the upper two levels of the system we see a ‘coupled’ localization for both 2D and 3D case. Here, the state in which majority of population will be found depends on the sign of the detunings between the upper levels and the intermediate level. The experimental implementation of the scheme using the D_2 line of Rb is also proposed.

I. INTRODUCTION

In recent years atom localization has received considerable attention owing to its potential applications in the areas of quantum information science [1], laser cooling and trapping of neutral atoms [2], Bose-Einstein condensation [3], atom nanolithography [4, 5] and microscopy [6]. Initial proposals for localizing atoms were confined to one dimension only. In this regard, many methods based on electromagnetically induced transparency (EIT) [1,7], coherent population trapping (CPT)[8,9] and stimulated Raman adiabatic passage (STIRAP) are suggested [10]. Recently, schemes have been proposed to localize atoms even in two and three dimensions. Ivanov and his collaborators have proposed a scheme for two dimensional (2D) atom localization by laser fields in a four-level tripod system [11]. Other schemes for 2D localization have also been proposed by Ding et.al.[12] and Wang et.al.[13]. Very recently, Ivanov’s group proposed a scheme for three dimensional atom localization in the same system[14]. Qi et al.[15] have proposed a scheme for 3D atom localization based on EIT. Clearly these new developments are going to open up numerous applications in many areas of science. For example, three-dimensional localization may be useful in high-precision position dependent chemistry [14]. In this work, we propose schemes to localize atoms both in two and three dimensions, via level populations, by using laser fields in an M-type five level atomic system.

II. MODEL

A standing wave pattern is created by four laser fields $\vec{E}_1, \vec{E}_2, \vec{E}_3$ and \vec{E}_4 . The electric field here is given by[16]

$$\vec{E}(\vec{r}, t) = \vec{E}_1^+(x)e^{-i\omega_1 t} + \vec{E}_2^+(y)e^{-i\omega_2 t} + \vec{E}_3^+(y)e^{-i\omega_3 t} + \vec{E}_4^+(x)e^{-i\omega_4 t} + cc. \quad (1)$$

The electric fields are such that \vec{E}_1 is a σ^- polarized wave with frequency ω_1 , \vec{E}_2 is a σ^+ polarized wave with frequency ω_2 , \vec{E}_3 is a π polarized wave with frequency ω_3 , \vec{E}_4 is again a σ^- polarized wave with frequency ω_4 .

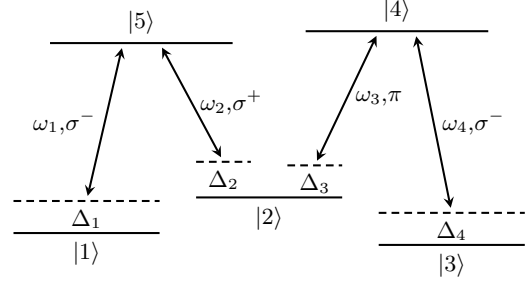


Figure 1. Configuration of electric fields for an M-type system. Here the electric fields form a standing wave pattern in a plane and atoms cross the plane in a direction perpendicular to the plane.

As shown in the Fig.(1), the upper levels are denoted by $|4\rangle$ and $|5\rangle$ and three ground levels by $|1\rangle, |2\rangle$ and $|3\rangle$. The transitions $|1\rangle \leftrightarrow |5\rangle, |2\rangle \leftrightarrow |5\rangle, |2\rangle \leftrightarrow |4\rangle, |3\rangle \leftrightarrow |4\rangle$ are driven by nearly resonant electric fields $\vec{E}_1(x) = \vec{E}_1 \sin(x), \vec{E}_2(y) = \vec{E}_2 \sin(y), \vec{E}_3(y) = \vec{E}_3 \sin(y), \vec{E}_4(x) = \vec{E}_4 \sin(x)$ respectively. The detunings[17] for these transitions are $\Delta_1 = \omega_1 - \omega_{51}, \Delta_2 = \omega_2 - \omega_{52}, \Delta_3 = \omega_2 - \omega_{42},$ and $\Delta_4 = \omega_3 - \omega_{43}$ respectively.

The coupling of the laser fields with the atom is given Rabi frequencies[17]

$$\begin{aligned} g_1(x) &= G_1 \sin(k_1 x) \\ g_2(y) &= G_2 \sin(k_2 y) \\ g_3(y) &= G_3 \sin(k_3 y) \\ g_4(x) &= G_4 \sin(k_4 x). \end{aligned} \quad (2)$$

where $G_j = |\vec{d}_j \cdot \vec{e}_j / \hbar|$ is coefficient of Rabi frequency and \vec{d}_j is dipole moment corresponding to j^{th} transition[17].

It is assumed that the center of mass of the atom is at rest, the interaction only affects the internal states and hence the Raman-Nath approximation[18] is valid. So in the interaction picture and rotating wave approximation (RWA)[19], the Liouville equation[20]

$$i\hbar\dot{\rho} = [\mathcal{H}, \rho] - i\gamma\rho \quad (3)$$

becomes

$$i\dot{\rho}_{11} = g_1(\rho_{15} - \rho_{51}) + i\gamma_1\rho_{55}, \quad (4a)$$

$$i\dot{\rho}_{22} = g_3(\rho_{24} - \rho_{42}) + g_2(\rho_{25} - \rho_{52}) + i\gamma_{52}\rho_{55} + i\gamma_{42}\rho_{44}, \quad (4b)$$

$$i\dot{\rho}_{33} = g_4(\rho_{34} - \rho_{43}) + i\gamma_3\rho_{44}, \quad (4c)$$

$$i\dot{\rho}_{44} = g_3(\rho_{42} - \rho_{24}) + g_4(\rho_{43} - \rho_{34}) - i\gamma_4\rho_{44}, \quad (4d)$$

$$i\dot{\rho}_{55} = g_1(\rho_{51} - \rho_{15}) + g_2(\rho_{52} - \rho_{25}) - i\gamma_5\rho_{55}, \quad (4e)$$

$$i\dot{\rho}_{12} = \rho_{12}(\Delta_{12} - i\Gamma_{23}) + g_3\rho_{14} + g_2\rho_{15} - g_1\rho_{52}, \quad (4f)$$

$$i\dot{\rho}_{13} = g_4\rho_{14} - g_1\rho_{53} + (\Delta_{1234} - i\Gamma_{13})\rho_{13}, \quad (4g)$$

$$i\dot{\rho}_{14} = -g_1\rho_{54} + g_3\rho_{12} + g_4\rho_{13} + (\Delta_{123} - i\Gamma_{14})\rho_{14}, \quad (4h)$$

$$i\dot{\rho}_{15} = g_1(\rho_{11} - \rho_{55}) + g_2\rho_{12} + (\Delta_1 - i\Gamma_{15})\rho_{15}, \quad (4i)$$

$$i\dot{\rho}_{23} = g_4\rho_{24} - g_3\rho_{43} - g_2\rho_{53} + (\Delta_{43} - i\Gamma_{23})\rho_{23}, \quad (4j)$$

$$i\dot{\rho}_{24} = g_3(\rho_{22} - \rho_{44}) + g_4\rho_{23} - g_2\rho_{54} + (\Delta_3 - i\Gamma_{24})\rho_{24}, \quad (4k)$$

$$i\dot{\rho}_{25} = g_2(\rho_{22} - \rho_{55}) + g_1\rho_{21} - g_3\rho_{45} + (\Delta_2 - i\Gamma_{25})\rho_{25}, \quad (4l)$$

$$i\dot{\rho}_{34} = g_4(\rho_{33} - \rho_{44}) + g_3\rho_{32} + (\Delta_4 - i\Gamma_{34})\rho_{34}, \quad (4m)$$

$$i\dot{\rho}_{35} = g_1\rho_{31} + g_2\rho_{32} - g_4\rho_{45} + (\Delta_{234} - i\Gamma_{35})\rho_{35}, \quad (4n)$$

$$i\dot{\rho}_{45} = g_1\rho_{41} + g_2\rho_{42} - g_3\rho_{25} - g_4\rho_{35} + (\Delta_{23} - i\Gamma_{45})\rho_{45}. \quad (4o)$$

Since ρ is a density matrix, we have $\rho_{ij} = \rho_{ji}^*$, $\sum \rho_{ii} = 1$. For the Δ s we have used following notation: $\Delta_{ijkl} = \Delta_i - \Delta_j + \Delta_k - \Delta_l$, $\Delta_{xyz} = \Delta_x - \Delta_y + \Delta_z$ and $\Delta_{mn} = \Delta_m - \Delta_n$. γ_1 and γ_3 are the decay rates which correspond to the relaxation 'into' ground states $|1\rangle$ and $|3\rangle$ respectively, γ_{52} is the decay rate that corresponds to the relaxation 'from' excited state $|5\rangle$ 'into' ground state $|2\rangle$, similarly other γ s are defined. Γ_{34} corresponds to the decay rate between states $|3\rangle$ and $|4\rangle$, similarly other Γ s are defined.

The decay rate between states $|1\rangle$ and $|2\rangle$, Γ_{12} , can safely be neglected because there is no field driving the transition and it is usually much smaller than the decay rates corresponding to driven transitions. Similarly other decay rates can be neglected. In effect we have

$$\Gamma_{12} \approx \Gamma_{13} \approx \Gamma_{14} \approx \Gamma_{23} \approx \Gamma_{35} \approx \Gamma_{45} \approx 0. \quad (5)$$

III. RESULTS AND DISCUSSION

2D Localization

As addressed by Ivanov[11], we take the two probe fields g_2 and g_3 to be weak so that in the long time we have g_2 and g_3 to be much smaller than g_1 , g_4 , Δ_2 , Δ_3 , Γ_{24} , Γ_{25} and other quantities of interest.

When the probe fields are weak, $g_2, g_3 \rightarrow 0$, we have most of the population in the state $|2\rangle$, hence $\rho_{22} \approx 1$ during the interaction of atom with the field. In the long time limit, we have $\dot{\rho}_{ij} = 0$. From these considerations we can obtain ρ_{44}, ρ_{55} from Eq.(4).

Considering Eq.(4f) in the long time limit and with weak probe fields g_2 and g_3 , we get

$$\rho_{21} \approx \frac{g_1}{\Delta_{12}} \rho_{25}. \quad (6)$$

Now we consider Eq.(4o). Near the nodes of g_2 , we get

$$\rho_{45} \approx \frac{g_3}{\Delta_{23}} \rho_{25}. \quad (7)$$

Putting Eq.(6) and Eq.(7) in Eq.(4l) along with $(\rho_{22} - \rho_{55}) \approx 1$, we have

$$\rho_{25} \approx \frac{g_2}{i\Gamma_{25} - (\frac{g_1^2}{\Delta_{12}} - \frac{g_3^2}{\Delta_{23}} + \Delta_2)}. \quad (8)$$

From Eq.(4a) and Eq.(4e), we get

$$\rho_{55} \approx \frac{ig_2(\rho_{25} - \rho_{52})}{\gamma_5 - \gamma_1}. \quad (9)$$

From Eq.(8) and Eq.(9), we get

$$\rho_{55} \approx \frac{2g_2^2\Gamma_{25}}{(\gamma_5 - \gamma_1)(\Gamma_{25}^2 + (\frac{g_1^2}{\Delta_{12}} - \frac{g_3^2}{\Delta_{23}} + \Delta_2)^2)}. \quad (10)$$

This expression gives the upper level population in state $|5\rangle$ in terms of Rabi frequencies g_1, g_2, g_3 . It is valid near nodes of g_2 and away from nodes of g_3 .

To obtain population in state $|4\rangle$, we consider Eq.(4j) in the long time limit and for weak g_2 and g_3 . We obtain

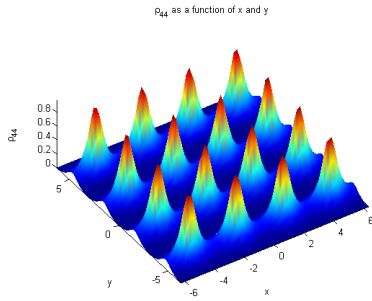
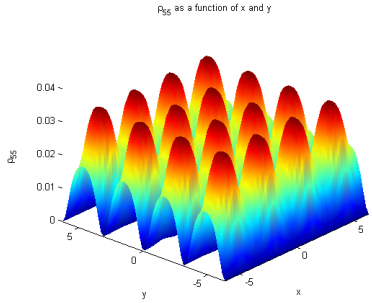
$$\rho_{23} \approx \frac{g_4}{\Delta_{34}} \rho_{24}. \quad (11)$$

Considering Eq.(4o) again. Near nodes of g_3 , we obtain

$$\rho_{54} \approx -\frac{g_2}{\Delta_{23}} \rho_{24}, \quad (12)$$

Putting $(\rho_{22} - \rho_{44} \approx 1)$ in Eq.(4k) and from Eq.(11) and Eq.(12), we get

$$\rho_{24} \approx \frac{g_3}{i\Gamma_{24} - (\frac{g_4^2}{\Delta_{34}} + \frac{g_2^2}{\Delta_{23}} + \Delta_3)}. \quad (13)$$

(a) Population in level $|4\rangle$ (b) Population in level $|5\rangle$ **Figure 2.** Population in states $|4\rangle$ and $|5\rangle$ as a function of (x,y) .

From Eq.(4c) and Eq.(4d), we get

$$\rho_{44} \approx \frac{ig_3(\rho_{24} - \rho_{42})}{\gamma_4 - \gamma_3}. \quad (14)$$

From Eq.(13) and Eq.(14), we have

$$\rho_{44} \approx \frac{2g_3^2\Gamma_{24}}{(\gamma_4 - \gamma_3)(\Gamma_{24}^2 + (\frac{g_4^2}{\Delta_{34}} + \frac{g_2^2}{\Delta_{23}} + \Delta_3)^2)}. \quad (15)$$

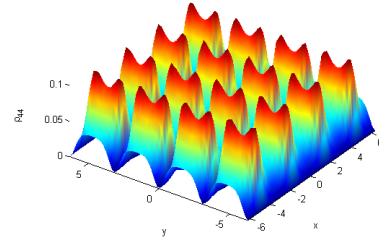
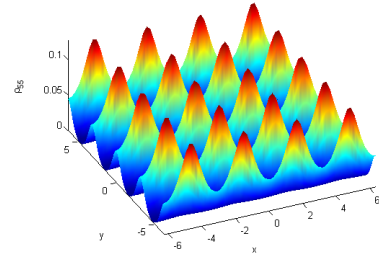
This expression gives the upper level population in state $|4\rangle$ in terms of Rabi frequencies g_2 , g_3 and g_4 . It is valid near the nodes of g_3 and away from nodes of g_2 .

Now we consider the case where all of the four fields are standing wave fields. We take g_1 , g_2 , g_3 and g_4 according to Eq.(2). For simplicity, consider $\gamma_5 - \gamma_1 = \gamma_4 - \gamma_3 = \gamma_0$, $\Delta_{12} = \Delta_{34} = \Delta_0$, $g_1 = g_4 = g_x$, $g_2 = g_3 = g_y$. We get

$$\rho_{44} \approx \frac{2g_3^2\Gamma_{24}}{\gamma_0(\Gamma_{24}^2 + (\frac{g_4^2}{\Delta_0} + \frac{g_2^2}{\Delta_{23}} + \Delta_3)^2)}, \quad (16)$$

$$\rho_{55} \approx \frac{2g_2^2\Gamma_{25}}{\gamma_0(\Gamma_{25}^2 + (\frac{g_1^2}{\Delta_0} - \frac{g_3^2}{\Delta_{23}} + \Delta_2)^2)}.$$

The population obtained from these expressions is shown in Fig.(2). For plotting purpose we take $\Gamma_{24} = 1.6\gamma_0$, $\Gamma_{25} = 1.4\gamma_0$, $g_2 = 4\gamma_0 \sin(k_2y)$, $g_3 = 4\gamma_0 \sin(k_3y)$, $g_1 = 6\gamma_0 \sin(k_1x)$, $g_4 = 6\gamma_0 \sin(k_4x)$, $\Delta = -6\gamma$, $\Delta_{23} = -2\gamma$, $\Delta_2 = 15\gamma$ and $\Delta_3 = 17\gamma$.

(a) Population in level $|4\rangle$ for g_2 as a cosine wave(b) Population in level $|5\rangle$ for g_2 as a cosine wave**Figure 3.** Phase shifted Population in states $|4\rangle$ and $|5\rangle$ as a function of (x,y) .

When fields are of the form Eq.(2), the localization patterns are according to Fig.(2) where most of the excited state population is localized in a single excited state depending on the sign of the detuning Δ_{23} . Instead if g_2 is of the form $g_2 = G_2 \cos(k_2y)$ while other three fields being of the form Eq.(2), we get a localization pattern where both the excited states are almost equally populated with different localization structures as shown in Fig.(3).

From Eq.(10) and Eq.(15) we see that the state where majority of population is localized depends *crucially* on the sign of the difference between detunings Δ_2 and Δ_3 i.e. on the sign of Δ_{23} . For a positive value of Δ_{23} , the excited state population localized in state $|4\rangle$ is much higher and is localized very tightly whereas for state $|5\rangle$, the population is low and area of localization is considerably larger. For $-\Delta_{23}$, excited state population is tightly and highly localized in state $|5\rangle$ whereas for state $|4\rangle$ the population is low and localized over a greater area.

In Fig.(4) it is observed from the contour plots that a greater population can be very tightly localized to a sub-wavelength region having an area of the order of $(\frac{\lambda}{5\pi})^2$ in state $|4\rangle$ whereas the range of localization in state $|5\rangle$ is approximately four times the former.

$$A_{loc}^{(4)} \approx \left(\frac{\lambda}{5\pi}\right)^2 \quad \text{and} \quad A_{loc}^{(5)} \approx \left(\frac{\lambda}{\frac{5\pi}{2}}\right)^2. \quad (17)$$

where $A_{loc}^{(4)}$ and $A_{loc}^{(5)}$ represent areas where population

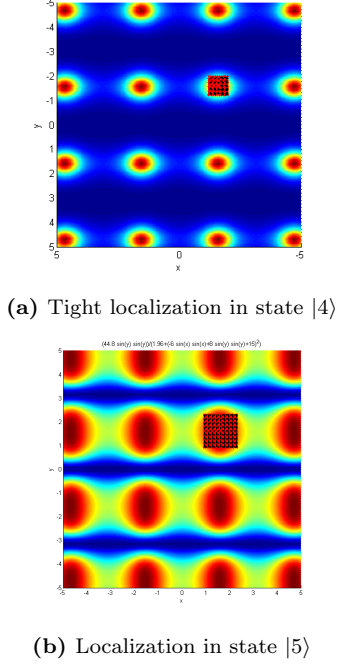


Figure 4. Large population can be tightly localized in state $|4\rangle$ within a region given by Eq.(17). Figure shows contour plot of Fig.(2a), red being the densest region. The red square at the top-left corner measures the area of the densest region in a peak.

can be localized in state $|4\rangle$ and $|5\rangle$ respectively.

3D localization

The scheme for localization of atoms in three dimensions is also presented below. The atomic states arrangement is same as Eq.(21) except that here two addition fields are required whose \hat{k} vectors are along \hat{z} and satisfy the selection rule Eq.(22). For the electric field configuration of the form

$$\begin{aligned} \vec{E}(\vec{r}, t) = & \vec{E}_1^+(x)e^{-i\omega_1 t} + \vec{E}_{21}^+(y)e^{-i\omega_{21} t} \\ & + \vec{E}_{22}^+(y)e^{-i\omega_{22} t} + \vec{E}_{31}^+(y)e^{-i\omega_{31} t} \\ & + \vec{E}_{32}^+(y)e^{-i\omega_{32} t} + \vec{E}_4^+(x)e^{-i\omega_4 t} + cc. \end{aligned} \quad (18)$$

the Rabi frequencies are given by

$$\begin{aligned} g_1(x) &= G_1 \sin(k_1 x), \\ g_2(y) &= G_{21} \sin(k_{21} y) + iG_{22} \sin(k_{22} z), \\ g_3(y) &= G_{31} \sin(k_{31} y) + iG_{32} \sin(k_{32} z), \\ g_4(x) &= G_4 \sin(k_4 x). \end{aligned} \quad (19)$$

where G_1, G_4 are of the form Eq.(2). The Rabi frequency G_{21} is given by $G_{21} = |\vec{d}_2 \cdot \vec{\epsilon}_{21} / \hbar|$. G_{22}, G_{31}, G_{32} are defined in the same way. Then the solutions of the Liouville

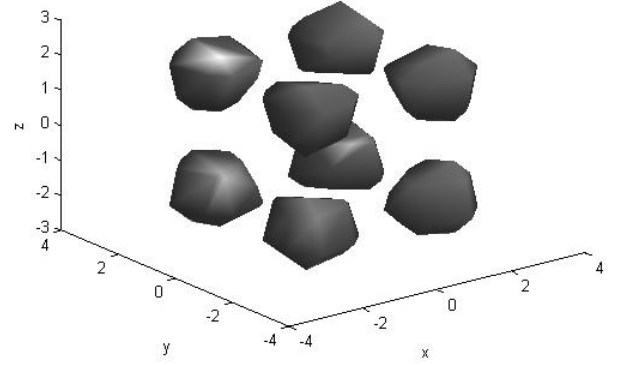


Figure 5. Plot for 3D localization of the population ρ_{44}

equation, Eq.(3), for the upper state population ρ_{44} and ρ_{55} are given by, in the long time limit, with RWA and in interaction picture,

$$\begin{aligned} \rho_{55} &\approx \frac{2|g_2|^2 \Gamma_{25}}{(\gamma_5 - \gamma_1)(\Gamma_{25}^2 + (\frac{g_1^2}{\Delta_{12}} - \frac{|g_3|^2}{\Delta_{23}} + \Delta_2)^2)}, \\ \rho_{44} &\approx \frac{2|g_3|^2 \Gamma_{24}}{(\gamma_4 - \gamma_3)(\Gamma_{24}^2 + (\frac{g_4^2}{\Delta_{34}} + \frac{|g_2|^2}{\Delta_{23}} + \Delta_3)^2)}. \end{aligned} \quad (20)$$

where $|\cdot|$ is the magnitude of the quantity. All the notations and approximations are same as that of Sec(II).

A simple plot for 3D localization of the population ρ_{44} is shown in Fig.(5). Here we take g_3 to be a constant/ running-wave pulse of the form $g_3 = G_3$, g_1 and g_4 to be sine waves along \hat{x} and g_2 to be along \hat{y} and \hat{z} . For plotting, we take $g_3 = 0.3\gamma$, $g_2^2 = 16\gamma^2(\sin^2(k_{21}y) + \sin^2(k_{22}z))$, $g_4 = 6\gamma \sin(k_4 x)$, $g_1 = 6\gamma \sin(k_1 x)$, $\Delta_{34} = 9\gamma$, $\Delta_{23} = 4\gamma$, $\Delta_3 = -12\gamma$, $\Gamma_{24} = 1.5\gamma$ and $\gamma_4 - \gamma_3 = \gamma_0$.

Implementation of 2D and 3D localization schemes using Rubidium

The model proposed in Section (II) can be practically implemented using the D_2 line of Rubidium atom where two upper levels are from $5^2P_{3/2}$ and three grounds levels are from $5^2S_{1/2}$ [21].

$$\begin{aligned} |1\rangle &= |5^2S_{1/2}, F = 1, m = +1\rangle, \\ |2\rangle &= |5^2S_{1/2}, F = 1, m = -1\rangle, \\ |3\rangle &= |5^2S_{1/2}, F = 1, m = 0\rangle, \\ |4\rangle &= |5^2P_{3/2}, F' = 1, m = -1\rangle, \\ |5\rangle &= |5^2P_{3/2}, F' = 0, m = 0\rangle. \end{aligned} \quad (21)$$

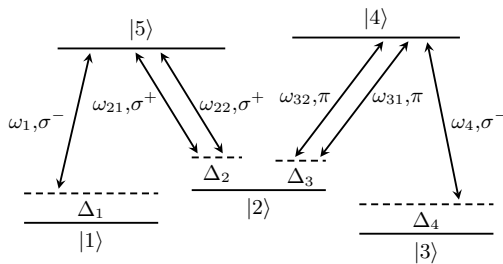


Figure 6. Configuration of electric fields for an M-type system for three dimensional localization.

The polarization of the laser fields driving this transitions should be in accordance with the selection rule. If

$$m_f - m_i = \begin{cases} +1 & \text{then } \sigma^+ \\ 0 & \text{then } \pi \\ -1 & \text{then } \sigma^- \end{cases} \quad (22)$$

The polarization of electric fields for the implementation of 2D localization scheme is also shown in Fig.(1). The 3D localization scheme can be implemented using Eq.(21) as well with addition of two extra laser fields. The setup is shown in Fig.(6).

CONCLUSIONS

In conclusion we have shown how to localize atoms in a M-type system in two dimensions as well as three dimensions. It is also pointed out that for 2D localization, the state in which majority of the population resides depends crucially on the sign of detuning Δ_{23} . Same conclusion is valid for three dimensions as can be easily seen from Eq.(20). We also estimated the range of localization numerically, Eq.(17). The effect of a phase shift of $\pi/2$ in making both the states almost equally populated with different localization structure is also studied. In the end, we also proposed a practical implementation of the two and three dimensional localization schemes using Rubidium atom.

* aksarma@iitg.ernet.in

- [1] A.V. Gorshkov, L. Jiang, M. Greiner, P. Zoller and M.D. Lukin, Phys. Rev. Lett. **100**, 093005 (2008).
- [2] H. Metcalf and P. Van der Straten, Phys. Rep. **244**, 203 (1994); W. D. Phillips, Rev. Mod. Phys. **70**, 721 (1998).
- [3] G. P. Collins, Phys. Today **49**, 18 (1996); Y. Wu and R. Cote, Phys. Rev. A **65**, 053603 (2002).
- [4] K. S. Johnson, J. H. Thywissen, W. H. Dekker, K. K. Berggren, A. P. Chu, R. Younkin, and M. Prentiss, Science **280**, 1583 (1998).
- [5] A. N. Boto, P. Kok, D. S. Abrams, S. L. Braunstein, C. P. Williams, and J. P. Dowling, Phys. Rev. Lett. **85**, 2733 (2000).
- [6] S. W. Hell, Science **316**, 1153 (2007).
- [7] D.D.Yavuz, N. A. Proite, Phys. Rev. A **76**, 041802 (2007).
- [8] G.S. Agarwal, K.T. Kapale, J. Phys. B **39**, 3437–3446 (2006).
- [9] H. Li, V.A. Sautenkov, M.M. Kash, A.V. Sokolov, G.R. Welch, Y.V. Rostovtsev, M.S. Zubairy and M.O. Scully, Phys. Rev. A, **78**, 013803 (2008).
- [10] J. Mompert, V. Ahufinger and G. Birkl, Phys. Rev. A, **79**, 053638 (2009).
- [11] V. Ivanov and Y. Rozhdestvensky, Phys. Rev. A **81**, 033809 (2010).
- [12] C. Ding, J. Li, X. Yang, D. Zhang, and H. Xiong, Phys. Rev. A **84**, 043840 (2011).
- [13] Z. Wang, B. Yu, J. Zhu, Z. Cao, S. Zhen, X. Wu and F. Xu, Annals of Physics **327**, 1132–1145 (2012).
- [14] V.S. Ivanov, Y.V. Rozhdestvensky and K.A. Suominen, arxiv: 1406.2156.
- [15] Y. Qi, F. Zhou, T. Huang, Y. Niu and S. Gong, J. Mod. Opt. **59**, 12, (2012).
- [16] R. J. Glauber, Phys. Rev. **130**, 1963.
- [17] H. J. Metcalf, P. van der Straten, Laser Cooling and Trapping, Springer, 1990.
- [18] Pierre Meystre, Atom Optics, Springer, 2001.
- [19] Christopher J. Foot, Atomic Physics, 2005.
- [20] Graham Thomas Purves, PhD Thesis, <http://etheses.dur.ac.uk/2663/>.
- [21] D. A. Steck, Rubidium 87 D Line Data, 2001.